ISSN 0036-0236, Russian Journal of Inorganic Chemistry, 2020, Vol. 65, No. 4, pp. 472–479. © Pleiades Publishing, Ltd., 2020.
Russian Text © The Author(s), 2020, published in Zhurnal Neorganicheskoi Khimii, 2020, Vol. 65, No. 4, pp. 449–457.

SYNTHESIS AND PROPERTIES OF INORGANIC COMPOUNDS

Synthesis of Calcium Carbonate in the Presence of Bile, Albumen, and Amino Acids

O. A. Golovanova[a], * and S. S. Leonchuk[a]

[a] *Omsk State University, Omsk, 644077 Russia*

**e-mail: golovanoa2000@mail.ru*

Received September 27, 2019; revised October 30, 2019; accepted November 28, 2019

Abstract—The thermodynamic and experimental modeling of calcium carbonate crystallization in a model solution of human bile is performed. $CaCO_3$ samples are synthesized in the presence of additives with variable additive concentrations. The phase and group-structure composition of the synthesized samples is determined by X-ray powder diffraction (XRD), Fourier-transform IR spectroscopy, and optical microscopy. Amorphous calcium carbonate and calcite are found to be primarily formed in the human bile model solution in the presence of glycine, glutamic acid, and albumen separately. When twenty amino acids and albumen are present in the highest concentrations permissible in the human body, vaterite is formed as the major phase. Distinctions in phase and group-structure compositions of samples are shown to occur depending on synthetic parameters. An effect is suggested to be caused by the compositions and concentrations of the additives used on the formation of a certain calcium carbonate polymorph.

Keywords: calcium carbonate, vaterite, aragonite, calcite, human bile, gallstones, crystallization, synthesis, phase composition

DOI: 10.1134/S0036023620040063

INTRODUCTION

Studies into the physicochemical conditions of calcium carbonate crystallization are an important task of modern science, despite the large amount of studies devoted to this compound [1–7]. The relevance of such studies is due to the widespread use of this mineral in many areas of modern science and technology. In particular, in ecology and meteorology in the near future it is planned to conduct an experiment to reduce the temperature of the Earth and eliminate the influence of greenhouse gases by spraying calcium carbonate particles reflecting sunlight into the stratosphere [8]. It is also known in paleontology and climatology to determine the age of various historical objects and the Earth's climate in different time periods of the past by the chemical and isotopic composition of calcium carbonate [9, 10].

More developed and currently no less relevant is the problem of mineral formation in the human body with the participation of calcium carbonate. Physicochemical reasons and features of this phenomenon, as well as the design of calcium carbonate based biocomposite materials are important issues of modern science [4, 11–15]. The role of this mineral is important in the formation of gallstones and the development of cholelithiasis, since this compound is part of choleliths and in some cases makes up most of them [5, 16, 17]. Gallstones also comprise cholesterol, bilirubin, and various other organic compounds [5]. In this case, cholesterol, phospholipids, proteins, amino acids and pigments in the bile can affect calcium carbonate crystallization and, as a consequence, the formation of gallstones [2, 5, 7, 16]. Importantly, cholelithiasis is currently a worldwide problem, since more than 10% of the world's population suffers from this disease, and the established rate of increase in incidence can increase this indicator to 20% as soon as by 2050 [18–20].

Polymorphism in calcium carbonate is known; calcium carbonate can exist in six polymorphs. These are crystalline calcite (a stable form), aragonite, and vaterite (both metastable); hydrates: monohydrocalcite and ikaite (hexahydrate); and amorphous calcite [7]. Of the gallstones formed in the human body, it is the metastable calcium carbonate polymorph that is formed to a greater extent, namely, vaterite (it is unstable when in a pure form; a monotropic phase transition to calcite occurs over time as the deposit ages in solution or under heating), because of its crystallization conditions [4, 5, 11, 21]. This feature of the phase composition of the inorganic component of choleliths is of interest, since its study can elucidate the true causes of gallstone formation and help in the development of new drugs and ways to prevent this disease.

To study the physicochemical conditions of crystallization and the phase composition of calcium car-

Table 1. Ion contents in bile [4]

Parameter	Value		
	min	avg	max
pH	6.5	7.25	8.0
C, mmol/L			
Na^+	130	205	280
K^+	2.7	8.85	15.0
Ca^{2+}	1.2	6.6	12.0
Mg^{2+}	1.3	2.15	3.0
Cl^-	14.5	70.25	126
HCO_3^-	8.0	31.5	55

bonate polymorphs formed in the real settings of the human body, it currently seems possible to use thermodynamic modeling methods [4, 22–24], as well as synthesis and characterization of the synthesized samples [12, 24–26]. To approximate the model being created to the real settings and to simulate its various states in this study, we use the concentrations of the substances in question such that are the norm for a healthy average person [5]. The variations of these concentrations may correspond to various pathological changes in the state of human bile.

This work is targeted at the thermodynamic and experimental modeling of calcium carbonate crystallization from a bile solution by varying the solution composition (precipitating ions, amino acids, albumen) and experimental parameters (concentrations of substances introduced into the system).

EXPERIMENTAL

Thermodynamic Modeling

To design a theoretical model of the formation of a solid phase in the Ca^{2+}–CO_3^{2-} system in human bile, we used a hypothetical solution where the content of inorganic macrocomponents, pH, ionic strength, and temperature corresponded to the average respective values for bile of an average adult and healthy person (Table 1) [4, 24]. The effect of organic components of bile on crystallization was not taken into account.

The theoretical characteristics of calcium carbonate formation as a solid phase in solution are the reference values of the solubility product at 298 K, reduced to 310 K according to the Van Goff isobar equation: $K^0_{sp,310}$ (vaterite) = 1.01×10^{-8} and $K^0_{sp,310}$ (calcite) = 2.72×10^{-9} [27, 28].

The conditional solubility products were calculated taking into account the activity coefficients of ions and the occurrence of protolysis and complexation of precipitate-forming ions (their mole fractions were calculated using the H_2CO_3 acidity constant at 310 K and the complexation function of Ca^{2+}, together with the stability constants of the considered complexes):

$$K_{sp}^{0\,cond} = \frac{K_{sp}^0}{\gamma_A^x \gamma_B^y x_A^x x_B^y}. \quad (1)$$

The activity coefficients were calculated by the Davies equation (in the Debye–Hückel model):

$$\log\gamma_i = -0.51 z_i^2 \left(\frac{\sqrt{I}}{1+\sqrt{I}} - 0.3I \right). \quad (2)$$

The possibility for the low-soluble compound A_xB_y ($CaCO_3$) to be formed in the considered system was quantified using supersaturation indices *SI*:

$$SI = \log\Omega = \log\left[\frac{a_A^x a_B^y}{\left(a_A^x a_B^y\right)_s} \right]^{\frac{1}{x+y}} = \log\left[\frac{a_A^x a_B^y}{K_{sp}^{0\,cond}} \right]^{\frac{1}{x+y}}. \quad (3)$$

All of the physicochemical processes occurring in the studied system were taken to be steady-state and isothermal ($T = 310$ K).

All necessary calculations were carried out in Microsoft Excel 2013 software, and the diagram was plotted in OriginPro 2018.

Synthesis of Calcium Carbonate

General synthetic scheme. Preserved medical bile (from SAMSON-MED, emulsion for topical application), a 250-mL sample, was divided into two equal portions (125 mL each). Then, the first portion was added with certain amounts of HCO_3^{2-} and an additive, and the second was added with Ca^{2+} (Table 2). After the added substances dissolved, the first solution with the additive was poured from a burette at a rate of ~0.15 mL/s to the second solution, which was thermostated in a beaker at 310 ± 1 K, under continuous stirring. After the mixing was complete, the thus-obtained solution (250 mL) was stirred for another 30 min. The precipitation occurred following the scheme

$$CaCl_2 + 2NaHCO_3 = CaCO_3 + 2NaCl + CO_2 + H_2O. \quad (3)$$

Syntheses in the presence of glycine and glutamic acid. The amounts of Ca^{2+} and CO_3^{2-} ions, glycine, and glutamic acid to be added were calculated from average Ca^{2+} and CO_3^{2-} concentrations in bile (Table 1) and average amino acid concentrations in human blood serum (Table S1) referred to 250 mL of the final solution [29].

$CaCO_3$ syntheses in the presence of albumen. The weight of albumen added was varied based on the average protein content in bile (from 0.025 to 0.14% on the whole, i.e., 0.083% by weight on the average) and in the doubled average concentration [5].

Table 2. Contents of major components and additives used in synthesis

Sample no.	Component, mol		Additive
	$CaCl_2 \cdot 2H_2O$	$NaHCO_3$	
1	1.65×10^{-3}	7.88×10^{-3}	Glycine, 6.25×10^{-5} mol
2			Glutamic acid, 2.86×10^{-5} mol
3			Albumen, 0.21 g
4			Albumen, 0.42 g
5	3.00×10^{-3}	13.8×10^{-3}	20 EAAs (according to Table 1) and albumen, 0.35 g

$CaCO_3$ synthesis in the presence of albumen and the twenty essential amino acids (EAAs). The amounts of $CaCl_2 \cdot 2H_2O$, $NaHCO_3$, and EAAs to be added were calculated with reference to the maximal values from Table 1 and Table S1, respectively, referred to the 250 mL of the final solution.

The resulting solutions were placed in a BIATRON thermostat cabinet maintained at 310 ± 1 K (human body's temperature) for 120 h. The thus-obtained precipitates were filtered, washed, and dried at room temperature until a constant weight was acquired and until chemically bound water was completely removed. Then, the solid phase was weighed and characterized by Z-ray powder diffraction, Fourier-transform IR spectroscopy, and optical microscopy. In total, five samples of solid calcium carbonate were obtained and analyzed in this way.

X-ray powder diffraction characterization of prepared samples was performed on a D8 Advance (Bruker) diffractometer. X-ray diffraction patterns were recorded in the range 5°–80° 2θ angles. The qualitative phase analysis of samples was carried out with reference to PDF-2 and with related literature [7, 30, 31].

IR spectra of solid phases were recorded on an FT-801 (Symex) spectrometer. A 0.5-mg powdery sample was mixed with 50 mg KBr and compacted into a disk-shaped tablet 3 mm in diameter at room temperature. The spectral resolution was 4 cm^{-1}; the total number of scans was 32. The spectra of tested samples were recorded in the range from 400 to 4000 cm^{-1}. The IR spectra were processed in software OriginPro 2018 and with reference to the literature data on the absorption peak positions for atomic groups [7, 25, 32, 33].

Optical microscopy served to study the morphology of solid particles using an XSP-104 (ARMED) microscope. Test samples were spread in thin layers over a glass slide, and the material was studied with a magnification of ×640. Micrographs were taken using Toup View software and equipment.

RESULTS AND DISCUSSION

The thermodynamic modeling of solid phase formation in the Ca^{2+}–CO_3^{2-} system initially ignored Ca^{2+} complexation but accounted only for the protolytic interactions of CO_3^{2-} for calcite and vaterite. The calcium carbonate stability field was rapidly designed as $pCa^{2+} = f(pCO_3^{2-}; pH)$. This was three-dimensional diagrams (surfaces) that described precipitation equilibrium at $SI = 0$, above which any figurative point of the system under study described its state as an ideal solution (no solid phase is formed; $SI < 0$), and below this surface, it describes the state where $SI > 0$ (a precipitate is formed). The diagram obtained for calcite appears in Fig. 1. No qualitative distinctions were found between the calcite and vaterite stability fields; however, all pCa^{2+} values obtained for vaterite are at a shift of about 0.35 to the negative side. This indicates that vaterite formation in a model solution requires higher concentrations of precipitate-forming ions than for calcite, the other conditions being equal. At pH 7.25 and $pCO_3^- = pHCO_3^- = 1.50$ (the mineral composition of human bile, Table 1), to the critical point (a point inside the stability field) for calcite, there corresponds $pCa^{2+} \approx 2.13$; for vaterite, $pCa^{2+} \approx 1.78$ [4, 24].

Because in reality calcium carbonate crystallization in bile can be affected by bile amino acids, we carried out analogous calculations taking into account Ca^{2+} complexation with glycine and glutamic acid (separately) using their average serum concentrations and with twenty essential amino acids referred to their maximal permissible serum concentrations (Table S1). The complexation function was calculated using the stability constants of Ca^{2+} with amino acids [34].

No qualitative changes were noticed upon the formation of a low-solubility compound ($CaCO_3$); accordingly, the stability field of glycine and glutamic acid in the concentrations created in the model solution remains unchanged. The decrease in pCa^{2+} corresponding to the critical point is less than 0.0005 units. In the same way, in case where the model solution is added with all EAAs in their highest concentration, no qualitative changes are observed. Even for pH 7.25 and

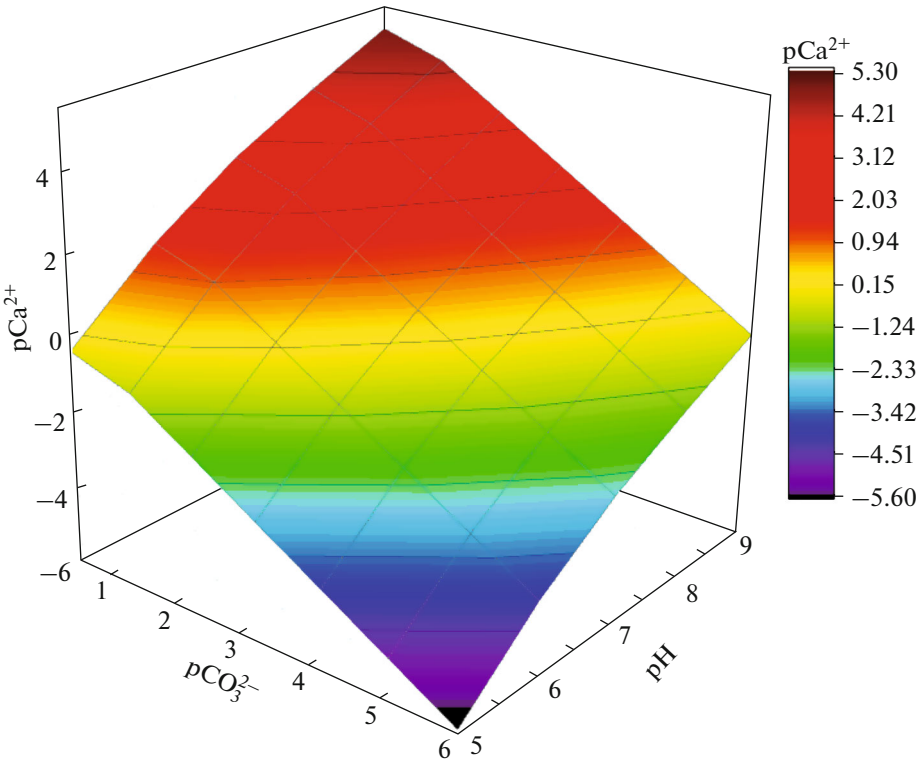

Fig. 1. Calcite stability field where Ca^{2+} complexation is ignored.

$pCO_3^- = pHCO_3^- = 1.50$, to the critical point in the diagram there corresponds $pCa^{2+} \approx 2.13$, a value as little as 0.003 pCa^{2+} units lower than the respective value in the absence of complexation; so the appearance of the $CaCO_3$ stability field is almost identical to Fig. 1.

The figurative point with the coordinates pH, 7.25; pCa^{2+}, 2.18; and $pHCO_3^-$, 1.50 describes the state of the human bile model solution with average respective values. This point lies above the stability field. For the point, $SI \sim -0.4$; that is, the system in this state is a true solution, which is, however, very close to precipitate–solution equilibrium state (especially in the case of calcite). So, equilibrium in the considered system could be shifted toward solid phase formation only when excessive Ca^{2+} and HCO_3^- ions would be added in concentrations equal to average physiological concentrations (Table 1), just as it was done during the subsequent synthesis of calcium carbonate.

The X-ray powder diffraction patterns of the prepared samples showed that the phase compositions of samples **1**–**4** almost do not differ from one another, while sample **5** has some distinctions. For clarity, Fig. 2 shows the diffraction patterns of samples **3** and **5**. One can see that sample **3**, prepared in the presence of albumen (0.083 wt %), features a broad band (extending from 15° to 55°) corresponding to amorphous $CaCO_3$ (the major phase) and peaks characteristic of minor calcite (23.0°, 29.4°), aragonite (26.3°), and monohydrocalcite (32.0°). In the X-ray diffraction pattern of sample **5**, the major phase is vaterite (21.0°, 24.9°, 27.0°, 32.7°, 44.5°, 49.0°, 50.0°, and 56.0°); peaks characteristic of minor calcite (29.4°, and 39.5°) are poorly defined [7, 30]. The peaks located at 21.7° and 20.3° and those to the left of them correspond to organic calcium salts and calcium compounds adsorbed on the $CaCO_3$ surface [35].

The FT-IR spectroscopic characterization of the prepared calcium carbonate samples correlates with XRD data. Powders **1**–**4** have nearly identical spectral patterns (Fig. 3). The IR spectra of these samples feature bands due to the C–C stretching vibrations at 1540–1580 cm^{-1} and narrow bands at 2850–2920 cm^{-1}, which correspond to the C–H stretching vibrations. These vibrations are characteristic of the presence of organic molecules in the powder in the form of calcium salts of organic acids and pigments that enter the bile or are adsorbed on the surface of crystallizing particles. The N–H stretching vibrations appearing as a broad band in the region of 3400 cm^{-1} correspond to the amino group vibrations in bilirubin, amino acids, or proteins adsorbed on the surface of calcium carbonate. The band at 1050–1100 cm^{-1} describes the O–H and C–N stretching vibrations, respectively, in bile pigments and bile cholesterol. The asymmetric stretching vibrations of C–O in CO_2 appear as a peak at 2350 cm^{-1}. The spectra also feature stretching vibra-

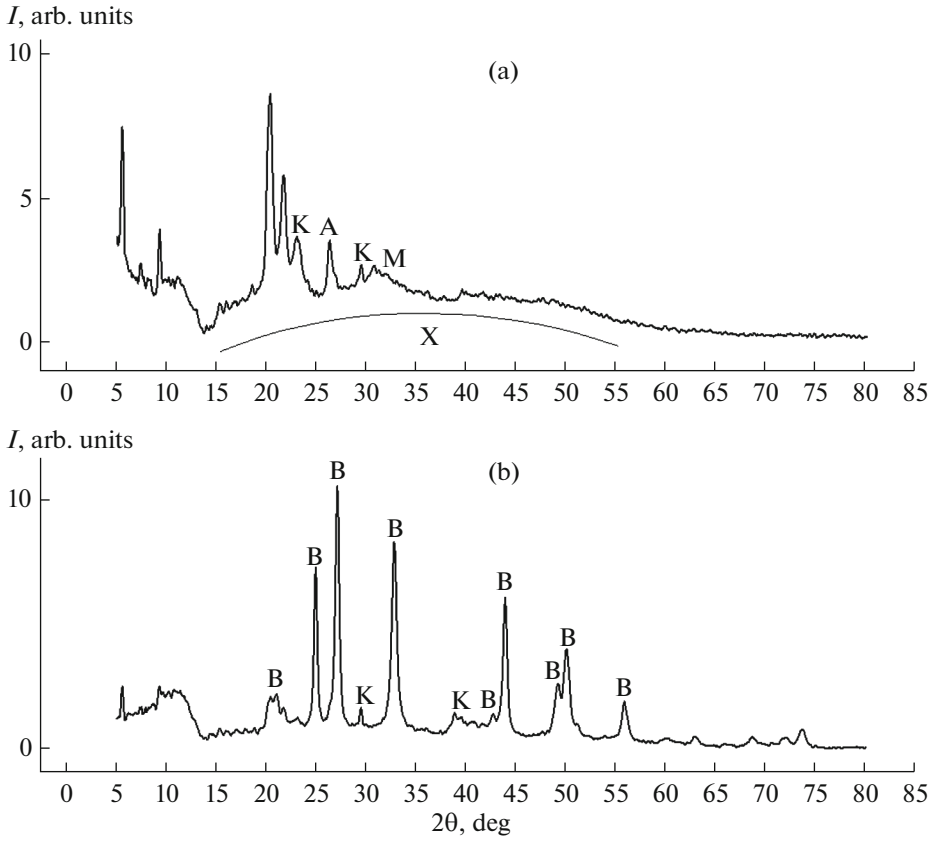

Fig. 2. X-ray diffraction patterns of (a) sample **3** and (b) sample **5**. Notations: A—aragonite, B—vaterite, C—calcite, M—monohydrocalcite, and X—amorphous calcium carbonate.

tions (at 1650 cm^{-1}) and bending vibrations (at 3740 cm^{-1}) in a water molecule. The spectra of four samples feature vibration bands of identical positions and intensities that correspond to a group of atoms in CO_3^{2-}. These are nondegenerate symmetrical changes in bond lengths ($\nu_1(CO_3^{2-})$) at 1068 cm^{-1}, doubly degenerate deformation of opposite bond angles ($\nu_2(CO_3^{2-})$) at 866–875 cm^{-1}, triply degenerate asymmetrical changes in bond lengths ($\nu_3(CO_3^{2-})$) at 1420–1475 cm^{-1}, and triply degenerate asymmetrical changes in one bond length in response to a change in bond angles ($\nu_4(CO_3^{2-})$) at 720 cm^{-1} [33]. This set of characteristic IR frequencies points to the presence of calcite and amorphous $CaCO_3$ in the samples [7].

So, no changes have been recognized in the group-structure composition among samples **1**–**4**. A comparison of samples **3** and **4**, which were prepared in the presence of various albumen concentrations, showed that a twofold increase in albumen concentration only insignificantly adds to the absorption intensity at 3400 cm^{-1} (N–H vibrations), indicating an enhancement of diverse interactions between albumen and calcium carbonate.

The spectrum of sample **5** has some distinctions from the samples considered above. At 2500 cm^{-1} a band appears corresponding to the S–H stretching vibrations in sulfur-containing amino acid molecules (cysteine, methionine), probably also adsorbed on the surface of the powder. The vibrations $\nu_3(CO_3^{2-})$ give a high-intensity band at 1440–1490 cm^{-1}, as distinct from those in the previously samples. At 875 cm^{-1} a well-defined $\nu_2(CO_3^{2-})$ vibration peak appears. The $\nu_4(CO_3^{2-})$ vibrations shift toward 745 cm^{-1}. The set of characteristic frequencies obtained for CO_3^{2-} indicates that sample **5** is represented by a vaterite phase [7].

The results of optical microscopy of the prepared powders are in agreement with the XRD and IR-spectroscopic data (Fig. 4). The morphology of the prepared crystals was compared to the literature data [7]; a similarity of particle shapes of calcium carbonate polymorphs was observed. For samples **1**–**4**, irregularly shaped crystals were observed, frequently grown together (such crystals are typical of amorphous $CaCO_3$), as well as cubic or rhombohedral crystals were observed in the mixture (calcite structure). Qualitative distinctions were noticed for sample **5**: its crys-

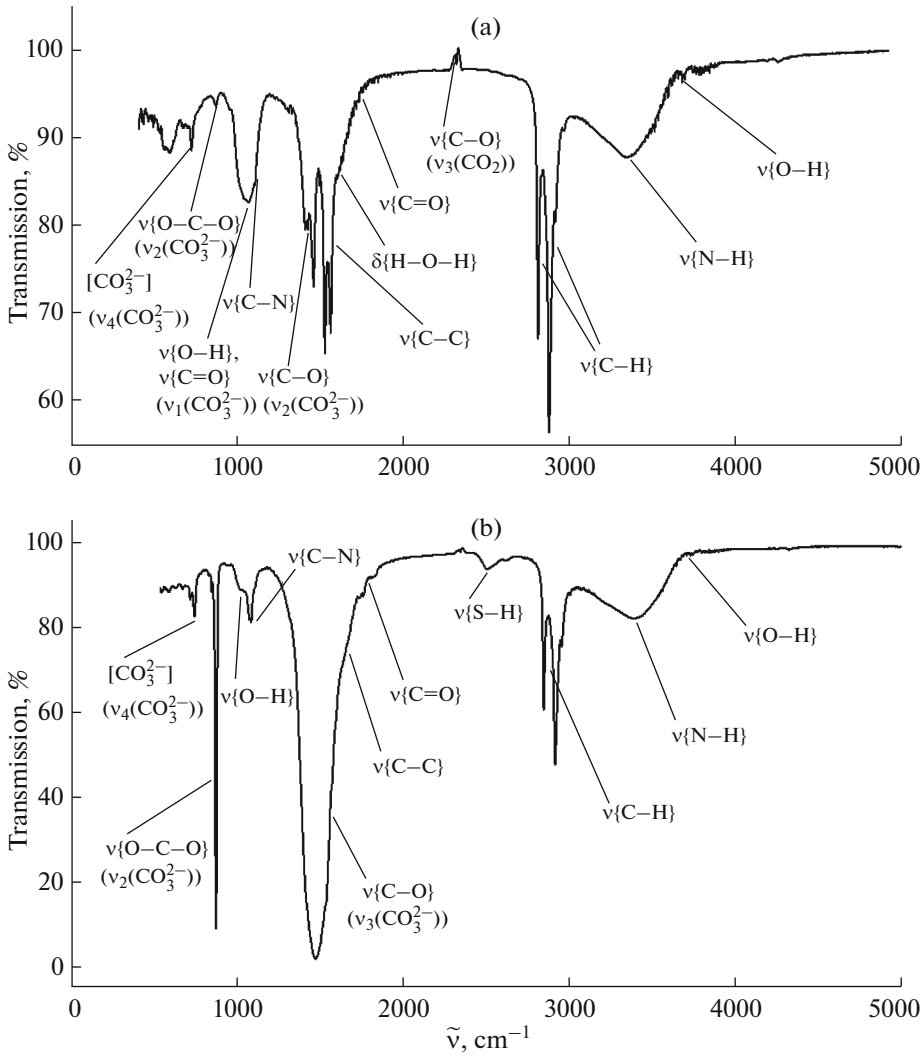

Fig. 3. IR spectra of (a) sample **3** and (b) sample **5**.

tals had spherical shapes (typical of vaterite), larger sizes and there were more of them.

Thus, from the results obtained by XRD, FT-IK spectroscopy, and optical microscopy, we may conclude that the nature and concentrations of additives to the bile, as well as the value of supersaturation of precipitate-forming ions, can affect the nature of crystallizing calcium carbonate phases. Qualitative changes in phase composition are observed in the presence of all EAAs and albumen in combination at their physiologically permissible highest concentration in human bile. Some researchers [36] observe that the presence of aspartic acid and cholesterol during calcium carbonate precipitation from aqueous solutions promotes vaterite formation along with calcite; when exposed to the solution for 96 h, however, the newly formed metastable vaterite almost completely converts to calcite, while in sample **5**, vaterite is represented as the major calcium carbonate phase and remains stable even after exposure to the model solution for 120 h. So we may suggest that the specific effect on phase formation and the stability of calcium carbonate is caused by some of the EAAs or a combination of several amino acids with one another, with albumen, or with bile components.

The results obtained in the work indicate the relevance and importance of studies of mineral formation in human bile on model systems to identify mechanisms, elucidation of functional relationships, and identification of the causes of gallstone formation.

CONCLUSIONS

Having performed thermodynamic and experimental modeling of calcium carbonate crystallization in a human bile model solution, we found that essential amino acids virtually have no effect on the formation of low-soluble compound ($CaCO_3$), but they yet change the qualitative phase composition of the

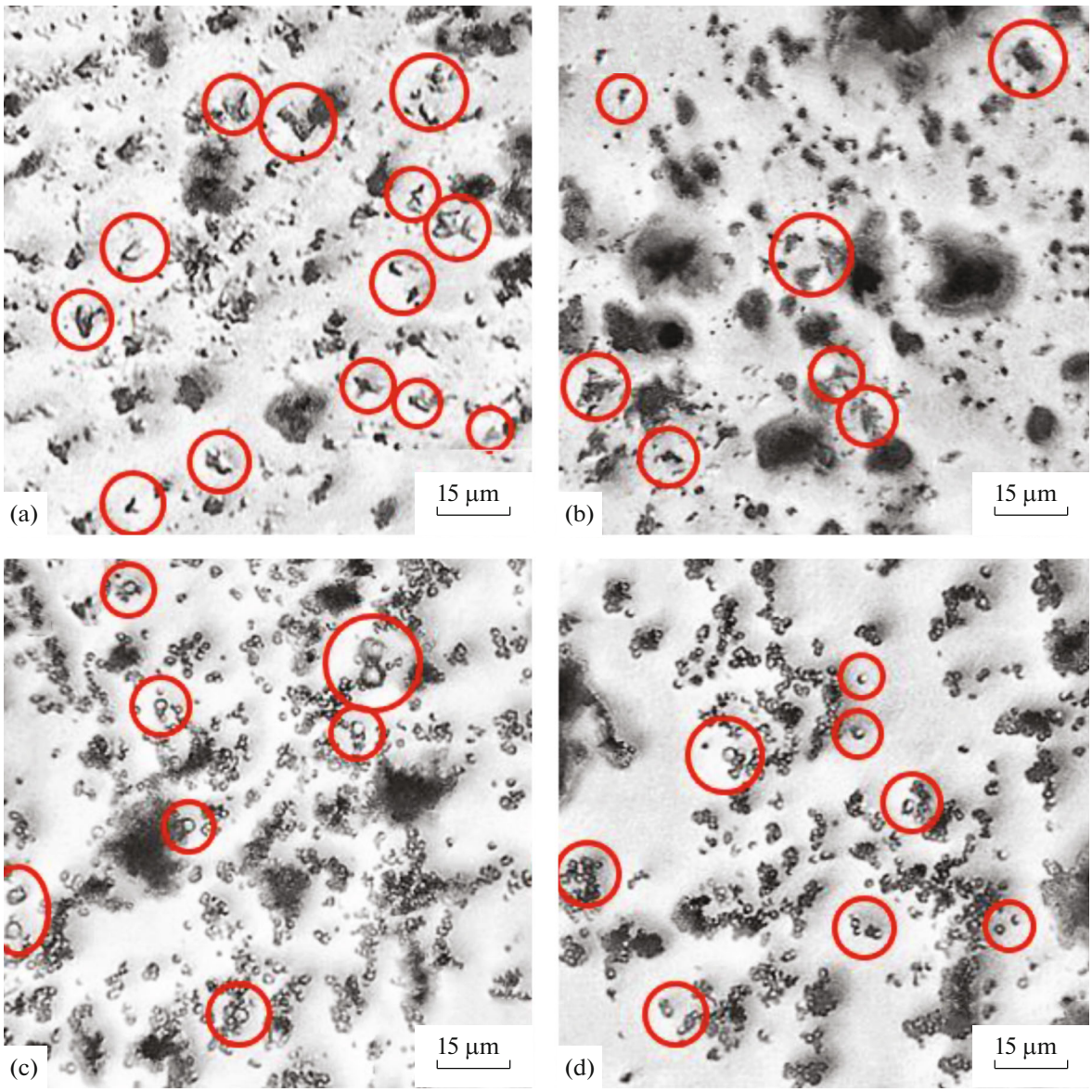

Fig. 4. Micrographs of (a, b) powder **3** and (c, d) powder **5**. Magnification: ×640.

resulting powders. When present in average physiological concentrations, glycine, glutamic acid, and albumen separately do not modify the composition of the synthesized samples relative to the calcium carbonate obtained in a purely bile model solution. However, when their concentrations increase to the highest values permissible for their joint presence, they enhance the formation of vaterite, the metastable calcium carbonate polymorph, as the major phase.

CONCLICT OF INTEREST

The authors declare that they have no conflicts of interest.

SUPPLEMENTARY MATERIALS

Supplementary materials are available for this article at https://doi.org/10.1134/S0036023620040063 and are accessible for authorized user.

Table S1. Contents of amino acids in human blood plasma [29].

REFERENCES

1. M. F. Butler, N. Glaser, A. C. Weaver, et al., Cryst. Growth Des. **6**, 781 (2006).
2. T. Lee and J. G. Chen, Cryst. Growth Des. **9**, 3737 (2009).
3. M. M. Tlili, M. B. Amor, C. Gabrielli, et al., J. Raman Spectrosc. **33**, 10 (2001).

4. S. S. Leonchuk and O. A. Golovanova, Vestn. Omsk. Univ. **42** (2), 66 (2019). https://doi.org/10.25513/1812-3996.2019.24(2).66-73
5. O. A. Golovanova, *Gallstones: A Monography* (Nauka, Omsk, 2012) [in Russian].
6. M. M. Kiselev, M. A. Vartanyan, S. V. Kirsanova, et al., Usp. Khim. Khim. Tekhnol. **29** (7), 41 (2015).
7. M. M. H. Al Omari, I. S. Rashid, N. A. Qinna, et al., *Profiles of Drug Substances, Excipients and Related Methodology*, Ed. by H. G. V. Brittain (Academic Press, Burlington, 2016). https://doi.org/10.1016/bs.podrm.2015.11.003).
8. J. Tollefson, Nature **563**, 613 (2018).
9. E. M. Griffith, A. Paytan, K. Caldeira, et al., Science **322**, 1671 (2008).
10. E. A. Vaganov, V. V. Kruglov, and V. G. Vasil'ev, *Natural Indicators of Climate Change: A Tutorial* (SFU Press, Krasnoyarsk, 2008) [in Russian].
11. E. V. Mashina, B. A. Makeev, and V. N. Filippov, Izv. Tomsk. Politekhn. Univ. **326** (1), 34 (2015).
12. O. A. Golovanova, Russ. J. Inorg. Chem. **63**, 1530 (2018).
13. O. A. Golovanova and E. S. Chikanova, Crystallogr. Repts. **60**, 970 (2015).
14. V. Korolkov, O. Golovanova, and M. Kuimova, *Biogenic–Abiogenic Interactions in Natural and Anthropogenic Systems*. https://doi.org/10.1007/978-3-319-24987-2
15. M. Acalovschi and F. Lammert, World Gastroenterol. News **17** (4), 6 (2012).
16. D. G. Tikhonov, Yakutsk. Med. Zh., No. 4, 91 (2015).
17. G. E. Njeze, Niger. J. Surg. **19** (2), 49 (2013).
18. Ya. M. Vakhrushev and N. A. Khokhlacheva, Arkh. Vnutr. Med. **29** (3), 30 (2016). https://doi.org/10.20514/2226-6704-2016-6-3-30-35
19. L. M. Stinton and E. A. Shaffer, Gut and Liver **6**, 172 (2012).
20. L. M. Stinton, R. P. Myers, and E. A. Shaffer, Gastroenterol. Clin. North Am. **39**, 157 (2010).
21. N. A. Pal'chik, V. N. Stolpovskaya, T. N. Moroz, et al., Russ. J. Inorg. Chem. **48**, 1921 (2003).
22. S. Vedantam and V. V. Ranade, Sadhana **38**, 1287 (2013).
23. M. Valavi, Master's Thesis (Limerick, 2016).
24. V. V. Korol'kov, Candidate Dissertation in Chemistry (Omsk, 2018).
25. T. V. Fadeeva and O. A. Golovanova, Russ. J. Inorg. Chem. **64**, 690 (2019).
26. R. R. Izmailov, O. A. Golovanova, Y. V. Tserikh, et al., Russ. J. Inorg. Chem. **61**, 817 (2016)).
27. A.-W. Xu Haynes, W.-F. Dong, M. Antonietti, and H. Colfen, Adv. Funct. Mater. **18**, 1307 (2008).
28. E. Koniqsberqer and L. Koniqsberqer, Pure Appl. Chem. **73**, 785 (2001).
29. A. Solodyankina, A. Nikolaev, O. Frank-Kamenetskaya, et al., J. Mol. Struct. **1119**, 484 (2016).
30. H. A. Almarshad, S. M. Badawy, and A. F. Alsharari, Comb. Chem. High Throughput Screen. **21**, 495 (2018).
31. S. Hayakawa, Y. Hajima, S. Qiao, et al., Anal. Sci. **24**, 835 (2008).
32. A. V. Strakhov and A. S. Gordetsov, Klin. Med. **2**, 86 (2012).
33. N. B. Egorov and V. V. Shagalov, *Infrared Spectroscopy of Rare and Disseminated Elements* (Tomsk, 2012) [in Russian].
34. O. A. Golovanova and I. A. Tomashevsky, J. Phys. Chem. **93**, 11 (2019).
35. M. Gonen, S. Ozturk, D. Balkose, et al., Ind. Eng. Chem. Res. **49**, 1732 (2010).
36. V. D. Franke and S. N. Bocharov, Proceedings of the XI Congress of the Russian Medicinal Society, St. Petersburg, 2010, p. 160.

Translated by O. Fedorova